



Distribution and environmental geochemical indices of mercury in tar contaminated beaches along the coast of Qatar

Ahmed Abou Elezz^{*}, Azenith Castillo, Hassan Mustafa Hassan, Hamood Abdulla Alsaadi, Ponnunony Vethamony

Environmental Science Center, Qatar University, Doha, P.O. Box 2713, State of Qatar

ARTICLE INFO

Keywords:

Qatar coast
Tarmat
Total mercury
Geochemical indices
BSAF

ABSTRACT

The current study aimed to gauge total mercury (THg) concentration and the environmental geochemical indices in tarmat contaminated sediments and test their presence in targeted coastal species. Layers of hard asphalt-like tarmats and sediment samples were collected from 34 sites along the coast of Qatar. The mean concentration of THg in tarmat-sediment mixture is $89 \pm 20 \text{ ng}\cdot\text{g}^{-1}$. THg concentration varies significantly between the northern and eastern coasts. Geographically, sampling area were divided into four zones according to the relative closeness with low to serious potential ecological risk index (E_p), moderate pollution load index (PLI), moderate Geoaccumulation index (I_{geo}), and no toxic risk (TRI) trending as Northern (Zones 4, 3) > North-Eastern (Zone 1) > Western (Zone 2) coasts. Three biota classes (*Gastropoda*, *Bivalvia*, and *Crustacea*) were sampled on the tarmat which the hermit crab (*Clibanarius signatus*) from Ras Rakan island obtained the highest THg ($977 \text{ ng}\cdot\text{g}^{-1}$) and BSAF (29.70).

1. Introduction

One of the pollutants that impacts the coastal environment of Qatar is the vast expanse of oil residue deposited on its beaches (Al-Kaabi et al., 2017; Arekhi et al., 2020; Rajendran et al., 2021; Veerasingam et al., 2020). After an oil spill, the oil stranded on the beach go through normal erosional, depositional and degradation processes affected by the beach hydrodynamic cycle, weather conditions e.g. temperature and seasonal wind patterns, therefore the oil would become buried, hardened, exposed, and mobilized several times (Michel et al., 2013). Oil can penetrate down to a few centimeters into the sediments forming a semi-cohesive oil/sediment matrix which is termed depending on their thickness – surface residue (SR) balls, <10 cm; SR patties, >10 cm and SR mats >20 cm up to 100s of m length (Arekhi et al., 2020; Michel et al., 2013; Rajendran et al., 2021; Veerasingam et al., 2020). The formation of marine tar residue is not a fully understood process, though various theories are put forward. The most widely accepted theory is surface-weathering (Goodman, 2003). It assumes that tarmats are weathered crude oil, whose volatile compounds were lost by evaporation, and the oil was turned into a soft brownish-black lump. Another theory states that during the weathering process, the emulsified oil interacts with suspended solids, sinks to the sea bottom, and forms an

immobile submerged oil mat, called tarmats (Hayworth and Clement, 2011). However, tarmats found on the coasts of Qatar are mostly exposed, except at select locations, where they are submerged during high tides. These weathered remnants are petroleum products derived from both natural and anthropogenic sources. The latter includes releases from oil exploration, consumption, and transportation, while naturally occurring seeps on the seafloor is a constant source of oil pollution (NAS, 2003). Globally reports indicate that more than half of marine tar loads result from anthropogenic activity, and the remaining can be attributed to natural sources (Warnock et al., 2015). Source identification is most often done by chemical fingerprinting to characterize the type of fuel and identify the concentration of compounds causing the contamination (Kruge et al., 2020). After the Gulf War oil spill of 1991, the northern to northwestern coast of Qatar was severely affected by tarmat contamination. This is the site where the UNESCO world heritage, Al Zubarah is situated. The chemical analyses of tarmat samples collected in 2015 in the study of Al-Kaabi et al. (2017), showed that the oils were from the Gulf War. This was also confirmed in the study of Arekhi et al. (2020) that the tarmat samples were identical to the Kuwaiti and Iraqi crude oil fingerprints similar to the source of the 1991 Gulf War oil spill. Multi-sensor satellite data was used to investigate two oil spill events (April to May 2014) in the Arabian Gulf and the

^{*} Corresponding author.

E-mail addresses: a.hassan@qu.edu.qa (A.A. Elezz), azenith@qu.edu.qa (A. Castillo).

<https://doi.org/10.1016/j.marpolbul.2022.113349>

Received 28 November 2021; Received in revised form 10 January 2022; Accepted 12 January 2022

Available online 29 January 2022

0025-326X/© 2022 The Authors. Published by Elsevier Ltd. This is an open access article under the CC BY license (<http://creativecommons.org/licenses/by/4.0/>).

Sea of Oman (near Al Khafji and Al Fujairah), covering a total area of 143.64 km² (Zhao et al., 2015). In 2017, Scanex Group for monitored the oil spills in the Arabian Gulf, covering the territorial waters and the exclusive economic zones of Saudi Arabia, Qatar, UAE, Iran, Iraq, and Kuwait. The number of detected oil spills from the discharges of tankers during 2017 was 4905, and this was distributed over an area of 13,835 km² (Scanex, 2018). Oil reaches the waters of Qatar from several anthropogenic sources such as routine operation of oil and gas exploration and exploitation, ship traffic in the Doha Port, Naval and Umm Said harbours, recreational boats, industrial discharges, atmospheric fallout, accidental oil spills and chronic releases from tankers bound from oil terminals in the northern part of the Arabian Gulf. An earlier study (Ossama Aboul Dahab, 1994) showed that the average quantity of tar found on the Arabian Gulf region beaches was in the range of 1–28,750 g·m⁻¹ (Table 1). The tarmat deposition rate was also estimated in the above study c. 100–600 g·m⁻¹ per month, and the variability can be attributed to the region's geomorphology, meteorological and hydrological conditions. The removal of tarmat is complicated without taking great care as the tarmat itself is a pollutant, and it is associated with various other contaminants. Mitigation is further complicated without destroying the natural habitat as the tarmats found had solidified and attached to the beach floor (Fig. 1). There had been previous reports of removal of tarmats, however recovery was found expensive, complicated to implement which mostly require extensive mechanical and manual exaction and sieving (Michel et al., 2013) but still did not necessarily result in a large recovery volume (Warnock et al., 2015).

The impacts of crude oil spills on the marine environment and spills within the Arabian Gulf have been reported in several studies and reviews, however, most of these studies were focused on the impacts of oil spills on the sediment and biota. In the studies of Farooqui et al. (2015) and Hoff et al. (2014) after the 1991 Gulf War oil spill, reported a remarkable impact of oil spills on mangrove habitats, including the death of young trees and seedlings, impairment of normal respiration and reducing the numbers of sentinels associated with oil-contaminated sediments. Other studies include investigation of total petroleum hydrocarbons (TPH), polyaromatics hydrocarbons (PAH), trace metals, and different forms of mercury (Bejarano and Michel, 2010; Freije and Awadh, 2009; Freije, 2015; Hassan et al., 2019). Mercury (Hg) analysis in crude oil and petroleum oil residues i.e. tar can be associated with many distinct problems as these samples are very complex and the Hg is found at very low concentrations that require the use of highly sensitive techniques (de Jesus et al., 2013). In multiple forms, mercury is present as a trace component of coal, crude oil, natural gas, gas condensates, tar sands and other bitumen (de Jesus et al., 2013; Wilhelm and Bloom, 2000) (Table 2). As a pollutant, Hg has been reported to affect the aquatic environment in a number of ways, from biodiversity to environmental health (Bejarano and Michel, 2010; de Jesus et al., 2013; Freije and Awadh, 2009; Freije, 2015; Hassan et al., 2019; Rocha et al., 2019; Wilhelm and Bloom, 2000). Wilhelm and Bloom (2000) reported Hg concentration in different crude oil and natural gas between 0.01 ng·g⁻¹ and 10,000 ng·g⁻¹.

Studies revealed that the concentration of Hg has significantly

Table 1
Average quantity of tar on the beaches of the Arabian Gulf Area.

Country	Concentration range (g·m ⁻¹)	Reference
Bahrain	14–858	(Fowler, 1985)
Oman	1–906	
United Arab Emirates	4–233	
Kuwait	5–2325	(Burns et al., 1982)
Saudi Arabia	0–28,750	(Coles and Gunay, 1989)
Qatar	58–>5000	(Ossama Aboul Dahab, 1994)

increased in the atmosphere, sea-dwelling mammals and birds in the vicinity of an oil spill, which affirmed the increased environmental risk posed by the release of Hg at oil spill areas (Otuya et al., 2008; Pandey et al., 2009; Pérez-López et al., 2006) (Table 3).

Our study found numerous species of marine crustacean and gastropods that inhabit in the vicinity of tarmats in the beaches of Umm Tais and Ras Rakan islands of Qatar (Fig. 1).

The review of the literature shows that reports on Hg in tarmats is scarce, instead most are on crude oil and associated products. Yun et al. (2013) and Pontes et al. (2013) reported that Hg concentration levels in crude oil from China and Brazil show a range of 13.4–1252.8 ng·g⁻¹. Bailey et al. (1961) stated that crude oil samples collected from Cymric fields, California yielded levels in the range of 1900–21,000 ng·g⁻¹, while tar samples, even though having lost their volatile hydrocarbon components, still showed very high values c.500 ng·g⁻¹. In the current study, we examined the concentration of THg in tar samples deposited on beach sediments and calculated its environmental geochemical indices including potential ecological risk, pollution load index, geoaccumulation index, and toxic risk index. Moreover, to estimate the proportion in which THg occurs in the various species of organisms that inhabits on the surface or are in the vicinity of tarmat contamination, the biota sediment accumulation factor (BSAF) was calculated.

2. Materials and methods

2.1. Study area

Tarmat samples deposited on beach sediments were randomly collected from 34 sites and each sample was analyzed in three independent replicates. There are in total 102 samples (34 × 3) along 120 km of the Qatar coast obtained from April 2018 to May 2019 (Fig. 2). The tarmats were littered on the shoreline including tar balls with a size ranging from 1 to 10 cm, while others were submerged. Moreover, some residual oils were observed on rock surfaces (refer to Fig. 1a, and b). Softer layers of oil samples were found under hard asphalt-like tarmats. A comprehensive study along the Qatar peninsula was performed to assess the THg contamination problem from the eastern coastline through the north and to the west beaches including mangroves area (Fig. 2). Table 4 shows all our sampling sites with GPS locations. Fig. 3 shows the collected tarmat samples. The samples were collected using a trowel and placed in an acid-washed glass jar. The samples were brought to the laboratory in Environmental Science Center, Qatar University (ESC, QU). Samples were freeze dried (AdVantage Pro-SP Scientific, USA) before analysis. The proportion of tar (asphaltene) and sediment were calculated in each sample to evaluate the deposition of the tar in beach sediments; however, the analysis was done on the tarmat-sediment mixture (refer to Fig. 3).

Adult sentinel species e.g., sand crab, bivalves, and gastropod were dwelling on the tarmats and its vicinity, however these species were only found in the north and northeast of Qatar. During Nov to Dec 2019 sampling, each five locations had different inhabitant species which *Lunella coronata* (Gmelin, 1791) a gastropod, *Asaphis* sp. a bivalve, *Clibanarius signatus* (Heller, 1861) a hermit crab, *Metopograpsus messor* (Forskål, 1775) the mangrove crab, *Leptodius exaratus* (Milne Edwards, 1834) a sand crab, *Barbatia setigera* (Reeve, 1844), and *Pirenella cingulata* (Gmelin, 1791) were identified (Table 5). The biota samples were transferred to icebox and transported to the ESC, QU laboratory. To avoid contaminations, the biota samples were thoroughly washed with distilled water. Muscle tissues were taken and freeze dried prior to THg analysis.

2.2. Total mercury (THg)

Total mercury concentrations in tarmat-sediment mixture and the muscle tissue of the sentinel species were analyzed by Cold Vapor Atomic Absorption Spectrometry (CVAAS) AULA-254 Gold (Mercury

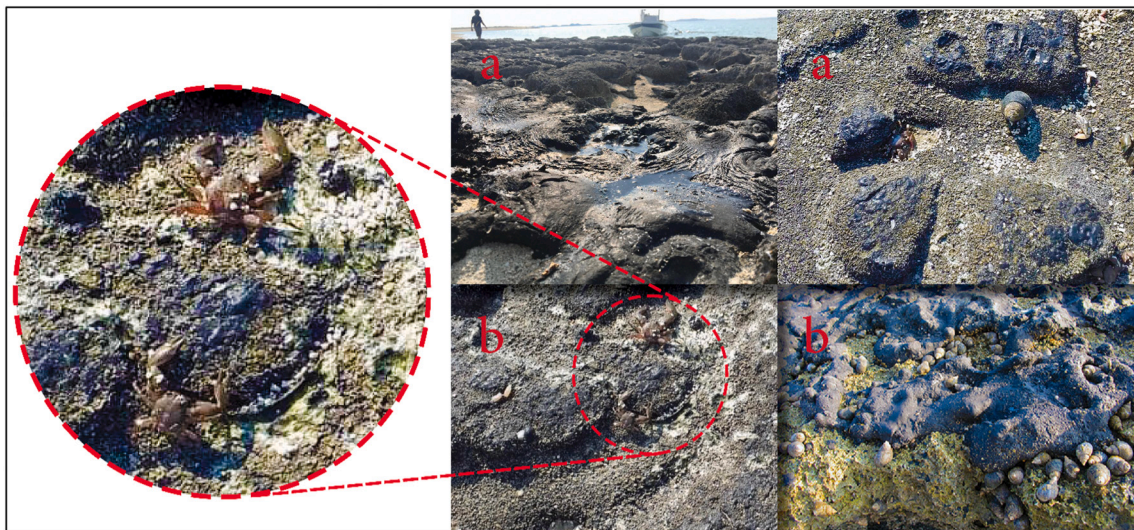


Fig. 1. Crab, gastropod, and bivalve species found on the tarmats in (a) Umm Tais and (b) Ras Rakan Islands.

Table 2
Concentration of Hg in fossil fuels and gas depends on geology.

Fossil fuels	Hg (ng·g ⁻¹)	Ref
Crude oil	1505	(Wilhelm and Bloom, 2000)
Utility fuel oil	0.67	
Petroleum condensate	76–105	
Asphalt	0.27	(de Jesus et al., 2013)

Table 3
Concentration ranges of Hg in atmosphere, biota, and seabirds before and after spill.

	Before spill (ng·g ⁻¹)	After spill (ng·g ⁻¹)	Ref
Atmosphere	1.76–3.2 ^a	7.34–20.4 ^a	(Pandey et al., 2009)
Biota	10,000–90,000	100,000–240,000	(Otuya et al., 2008)
Seabirds	ND	12,803	(Pérez-López et al., 2006)

^a Concentration of Hg in (ng·m⁻³).

Instruments GmbH, Germany) running with the AULA-254 program (AULA-WIN, TM based) for data processing and equipped with mercury UV-absorption source set at 253.7 nm wavelength (Elezz et al., 2018). In essence, 0.5 ± 0.05 g (dry weight) of freeze-dried homogenized samples were accurately weighed into a 50 ml Teflon tube. Samples were then subjected to microwave (Mars 6, CEM Corporation, USA) acid digestion using 1 ml HF, 5 ml HNO₃ (Suprapur, Merck, Germany) and 3 ml H₂SO₄ (98%, AnalaR, Scott Science UK, United Kingdom). The microwave was set for 30 min at 200 °C and 280 psi pressure. The digested samples were diluted using ultra-pure water to 50 ml (Barnstead Nanopure, Thermo Scientific, UK). Aliquot sample of 10 ml was further treated, as per Wilhelm and Bloom (2000), with Tin (II) chloride, hydroxyl ammonium hydrochloride, and potassium permanganate solutions (max 0.000001% Hg, Merck KGaA, Germany) to complete the oxidative process. Each sample was analyzed in three replicates.

2.3. Potential ecological risk index

The potential ecological risk index (E_r) were used to evaluate the hazard level of (Hg) in the sediments (Dash et al., 2021; Guo et al., 2010) along the Qatari coasts. The formula of potential ecological risk index (E_r) is:

$$E_r = C_f \times T_r \quad (1)$$

where (C_f) is the contamination factor that used to evaluate the pollution of Hg in sediment; (T_r) is the response coefficient of Hg, the response coefficient of mercury (T_r) is equivalent to 40 and reflects the toxicity of mercury on the ecosystem (Guo et al., 2010). Based on their strengths, the contamination levels can be classified into low risk ($E_r < 40$), moderate ($40 \leq E_r < 80$), higher ($80 \leq E_r < 160$), high ($160 \leq E_r < 320$), and serious risk ($E_r \geq 320$). The equation used to calculate the contamination factor of Hg is:

$$C_f = \frac{C_{heavy\ metal}}{C_{background}} \quad (2)$$

where $C_{heavy\ metal}$ is used to measure the mercury concentration in sediments, and $C_{background}$ is the reference value of mercury based on the upper limits of Hg background values. From the previous baseline study of Hassan et al. (2019) in Qatar's coastal marine zone, this value is set as 34 ng·g⁻¹.

The contamination levels can be categorised on a scale ranging from 1 to 6 as follow: low ($C_f < 1$), moderate ($1 \leq C_f < 3$), considerable ($3 \leq C_f < 6$), and very high degree ($C_f \geq 6$) (Islam et al., 2015).

2.4. Pollution load index (PLI)

The pollution load index is determined based on Eq. (3). It illustrates the particular site or zone's overall pollution by representing its state of toxicity (Angulo, 1996; Dhamodharan et al., 2019). It is categorised (PLI ≤ 1) as sites having no pollution, (1 ≤ PLI ≤ 2) slight pollution, (2 ≤ PLI ≤ 3) moderate pollution, or highly polluted (PLI > 3) (Liu et al., 2016a, 2016b).

$$PLI = \sqrt[n]{C_{f1} \times C_{f2} \times \dots \times C_{fn}} \quad (3)$$

where C_f indicates the contamination factor for mercury in each sampling site and (n) is equal to 1 due to a single element (Hg).

2.5. Geoaccumulation index (I_{geo})

Geoaccumulation index is used to evaluate heavy metal pollution of sediments based on the background level of natural and anthropogenic variations, and is calculated according to Müller, 1969.

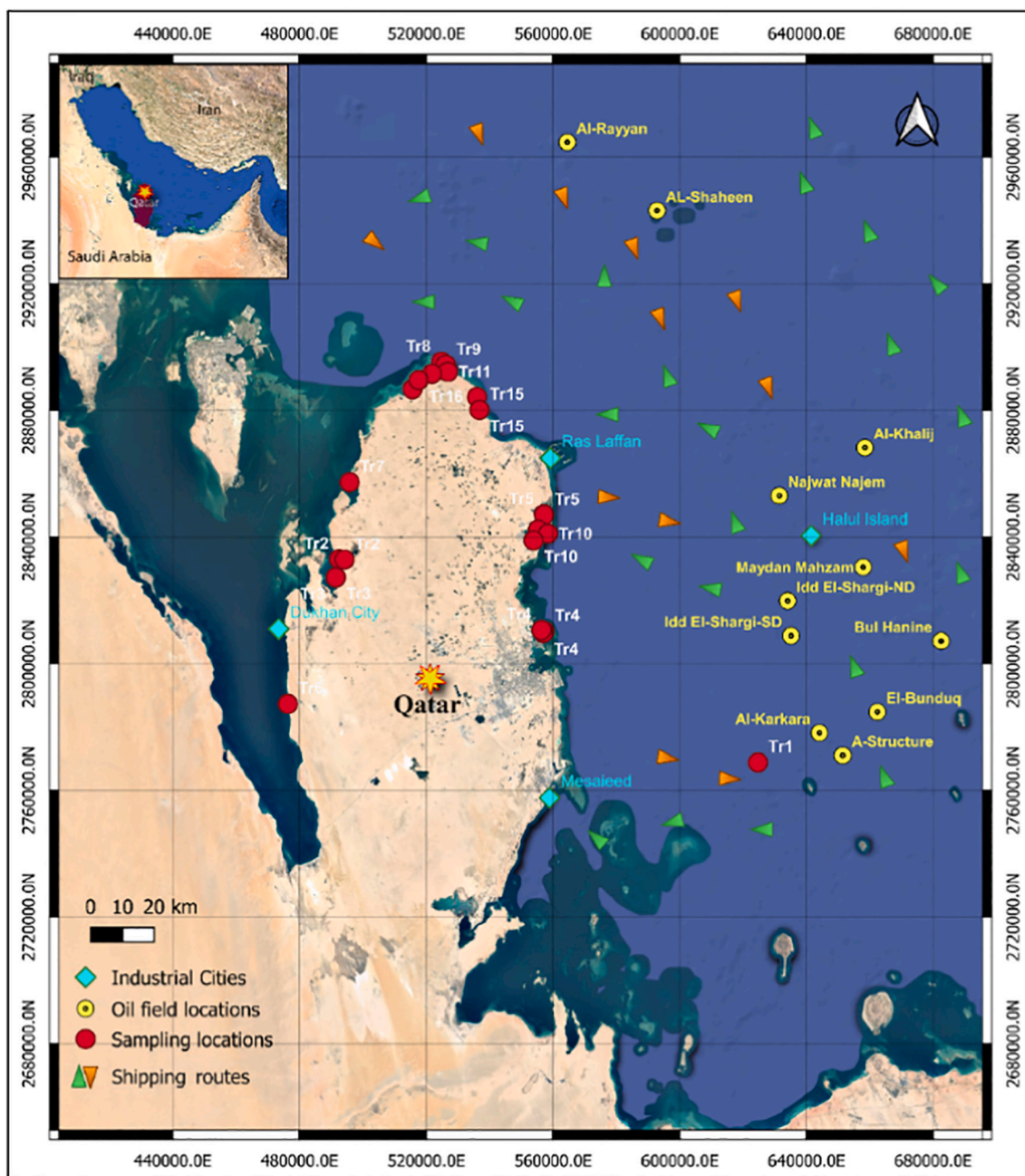


Fig. 2. Sampling locations including shipping routes, oil fields, and industrial areas along the Qatar coast (<https://www.qp.com.qa/>), (<https://shippingwatch.com>) (Qatar Petroleum, 2019).

$$I_{geo} = \log_2 \left[\frac{C_n}{1.5 B_n} \right] \tag{4}$$

where I_{geo} pollution index in sediment, C_n mercury concentration in sediments, and B_n is the background of mercury in sedimentary shales ($0.4 \text{ ng}\cdot\text{g}^{-1}$) (Wedepohl, 1961), and multiplied by 1.5 as a correction coefficient. I_{geo} differentiated pollution degree into 6 classes from ≤ 0 to ≥ 5 . It is categorised ($0 < I_{geo} < 1$) as unpolluted, ($1 < I_{geo} < 2$) as unpolluted to moderately polluted, ($2 < I_{geo} < 3$) as moderately polluted, ($3 < I_{geo} < 4$) as moderately to strongly polluted, ($4 < I_{geo} < 5$) as strongly polluted, ($I_{geo} > 5$) as strongly to extremely polluted (Ranjbar Jafarabadi et al., 2017).

2.6. Toxic risk index

The total risk index (TRI) method considers heavy metals' PEL and TEL effects for toxic risk evaluation in sediments (Zhang et al., 2016). The following formula can be used to evaluate the (TRI) of the heavy metal(s) under consideration (Hg) in sediment.

$$TRLi = \sqrt{\left(\frac{C_i}{TEL}\right)^2 + \left(\frac{C_i}{PEL}\right)^2} \tag{5}$$

where ($TRLi$) is the toxic risk index of a specific heavy metal, (C_i) is the metal concentration in sediments, Threshold Effects Level (TEL) and (PEL) the Probable Effects Level. The pollution level of TRI characterized according to Ranjbar Jafarabadi et al. (2017) as following: no toxic risk ($TRI < 5$), low toxic risk ($5 < TRI < 10$), moderate toxic risk ($10 <$

Table 4
Coordinates and symbols of sampling locations.

S. No	Location	Location symbol	Latitude (°N)	Longitude (°E)	S. No	Location	Location symbol	Latitude (°N)	Longitude (°E)
1	Sharao Island	Tr1	25.03038	52.235983	19	Al Khor1	Tr10	25.66743	51.53657
2	Abu Feleita Island (1)	Tr2	25.61483	50.924967	20	Al Khor2	Tr10	25.69855	51.55093
3	Abu Feleita Island (2)	Tr2	25.61363	50.9422	20	Al Khor Ras-Matha Area	Tr10	25.68685	51.58217
4	Kwasan (1)	Tr3	25.56332	50.915183	21	Al Khor Girl Scout	Tr10	25.66738	51.53653
5	Kwasan (2)	Tr3	25.56265	50.914533	22	Al Mafjar	Tr11	26.14862	51.26827
6	Al Aliya Island - East	Tr4	25.40853	51.569717	23	Al Ghariya1	Tr12	26.07627	51.36008
7	Al Aliya Island - West	Tr4	25.404	51.565883	24	Al Ghariya2	Tr12	26.07623	51.36003
8	Al Aliya Island - North	Tr4	25.4118	51.560167	25	Al Jumail (1)	Tr13	26.1	51.15615
9	Umm Al Far - North	Tr5	25.74147	51.56955	26	Al Jumail (2)	Tr13	26.09942	51.15653
10	Umm Al Far - South	Tr5	25.73958	51.570217	27	Ruwais old	Tr14	26.14317	51.2182
11	Umm Bab	Tr6	25.20207	50.765133	28	Ruwais1	Tr14	26.14313	51.21818
12	Umm Al amah	Tr7	25.8344	50.95815	29	Ruwais2	Tr14	26.14315	51.21817
13	Ras Rakan - Shoreline South	Tr8	26.17753	51.2481	30	Fuwairit	Tr15	26.0403	51.36763
14	Ras Rakan - South	Tr8	26.17738	51.24745	31	Fuwairit	Tr15	26.04025	51.36768
15	Ras Rakan - South Soft	Tr8	26.17747	51.24805	32	Fuwairit	Tr15	26.04028	51.36767
16	Umm Tais1	Tr9	26.16863	51.260733	33	Abu Al Dhalof (1)	Tr16	26.1248	51.17618
17	Umm Tais 2	Tr9	26.1689	51.261467	34	Abu Al Dhalof (2)	Tr16	26.12518	51.17603
18	Umm Tais 3	Tr9	26.16897	51.261517					

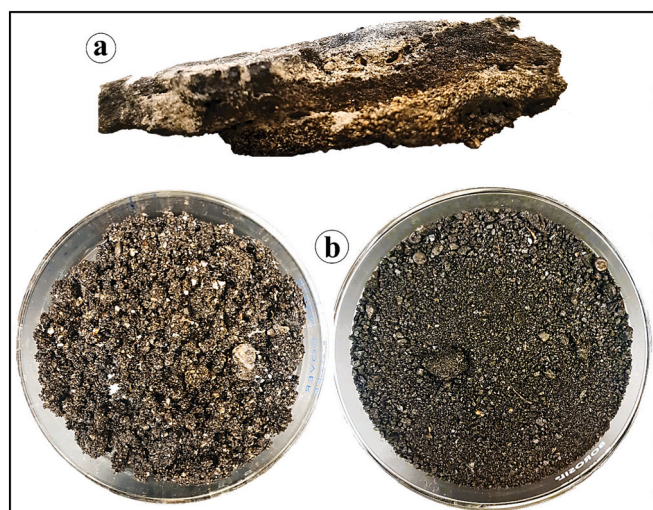


Fig. 3. (a) Layer of sand and tar; (b) samples of collected tar: freeze-dried and ground.

Table 5
Location and coordinates of biota samples collected during Nov-Dec 2019.

Species	n	S. No.	Location	Latitude (°N)	Longitude (°E)
<i>Lunella coronata</i>	5	14	Ras	26.17738	51.24745
<i>Asaphis</i> sp.	16		Rakan		
<i>Clibanarius signatus</i>	50	15	Ras	26.17747	51.24805
<i>Metopograpsus messor</i>	7		Rakan		
<i>Clibanarius signatus</i>	40	16	Umm Tais	26.16863	51.260733
<i>Leptodius exaratus</i>	5				
<i>Barbatia setigera</i>	4	17	Umm Tais	26.16890	51.261467
<i>Pirenella cingulata</i>	25	22	Al Mafjar	26.14862	51.26827

TRI < 15), considerable toxic risk (15 < TRI < 20), very high toxic risk (TRI > 20).

2.7. Biota sediment accumulation factor

Biota Sediment Accumulation Factor (BSAF) is used to describe

bioaccumulation of sediment contaminants in aquatic food webs between both the sediment and organism (Ghosh et al., 2020), which in this study, Crab, Bivalvia and Gastropoda organisms were used. The BSAF is the ratio between concentration of the analyte(s) (THg) in the organism muscle tissue ($\text{ng}\cdot\text{g}^{-1}$, dry weight) and its concentration in the surrounding medium (tar-sediment mixture) in $\text{ng}\cdot\text{g}^{-1}$, dry weight. BSAF was calculated according to Ghosh et al. (2020), Ziyaadini et al. (2016), ECHA (2012) and Mohamed and Mohamed (2005) as follow:

$$BSAF = \frac{\text{Metal concentration in organism}}{\text{Metal concentration in surrounding medium}} \quad (6)$$

According to BSAF values, organisms were classified as either, macroconcentration if the $BSAF > 2$; microconcentrator if the $1 < BSAF < 2$; or deconcentrator if $BSAF < 1$ (Nenciu et al., 2016; Ziyaadini et al., 2016).

2.8. Quality assurance and quality control (QA/QC)

Analytical quality assurance was established by analysis of reagent blanks and certified reference materials (CRM). Two CRMs were used: (i) Trace Elements in Mussel Tissue (NIST-2976) sourced from the National Institute of Standards and Technology, and (ii) Marine Sediment Certified Reference Material for Trace Metals (PACS3) obtained from National Research Council of Canada. The QC samples have constituted 10% of the total analyzed samples to obtain a sufficient quality. All samples were analyzed in triplicate with an average weight of 0.25 ± 0.05 g. Table 6 provides the obtained concentration and percentage recovery in addition to the limit of detection (LOD) and limit of quantification (LOQ).

Table 6
Detailed QA/QC information including (LOD), (LOQ), Certified values, Measured values, and Recovery (R%).

Analysis items	THg	
	Sediment ($\text{ng}\cdot\text{g}^{-1}$)	Biota ($\text{ng}\cdot\text{g}^{-1}$)
LOD	0.01	0.01
LOQ	0.04	0.04
CRMs	PACS 3	NIST-2976
Certified values	2980 ± 360	61.0 ± 3.6
Measured values	2850 ± 340	67.0 ± 2.1
R%	96	109

2.9. Data analysis

The sampling locations were grouped according to their similarities in THg contamination using Ward Linkage-Euclidean Distance clustering method. The data obtained were analyzed using one-way analysis of variance (ANOVA) with post hoc Tukey's HSD, and Pearson correlation between variables (bivariate correlation) using IBM-SPSS statistics 25 software. All data were tested for normal distribution (Shapiro-Wilk) before applying the ANOVA, otherwise a non-parametric Kruskal-Wallis ANOVA and Mann-Whitney post hoc was used to find out any significant variation between concentrations in samples from different stations with 95% confidence level. Pearson correlation and independent *t*-tests was also used to delineate relationship between groups of THg levels in biota and tarmat-sediment mixture samples.

3. Results and discussion

The observed tarmats were highly weathered that looked like asphalt indicative of a solidified old oil spill; although there were few soft melted rubbery textures which both could have resulted from the extreme warm temperature of Qatar, or the oil source might have been at different timing. The tarmat deposits in the Qatari coasts were observed largest with an average of $9.25 \text{ g}\cdot\text{m}^{-1}$ in the north of the country (Veerasingam et al., 2020) which were likely from the three-decade old oil spill of 1991 Gulf War (Arekhi et al., 2020). In the study from the tar remnants of the Deepwater Horizon oil spill of Gulf of Mexico, U.S.A., the tar residues contained 87.2–95.8% of sand and shells which were relatively unweathered oil that formed due to sinking and sedimentation rather than primarily surface weathering (Hayworth and Clement, 2011; Michel et al., 2013). In our study, the sediment fraction ranged from 12 to 75% while the tar (asphaltenes) fraction ranged from 25 to 88% which some were deposited up to 15 cm on top of the sediments (refer to Figs. 1 and 3). The difference in tarmat-sediment fractions could be attributed to the different rate of oil stranding which is

influenced by wind deflation, sand migration, beach accretion and bathymetry (Michel et al., 2013). As stated earlier, there is limited study on the estimate of THg concentration in tarmats and the biota inhabiting or in the vicinity of tarmats from any region in the Gulf Cooperation Countries (GCC). To fill this knowledge gap, the data below is presented and since the samples obtained in this present study is a mixture of sediment and tar, the concentrations will be compared against the levels of these pollutants in sediments and in petroleum crude and related products.

The dataset was subjected to the Ward Linkage-Euclidean Distance clustering method to predict the site similarities according to their relative closeness. The obtained dendrogram (Fig. 4a) showed four distinct zones (clusters). Zone 1 (East of Qatar) covered sites 1, 4, 5, 6, and 11; Zone 2 (West of Qatar) consisted of sites 2, 3, 7, and 8; Zone 3 (North of Qatar) included sites 9, 10, 12, 15, 16, and 20, and the rest of the sites comprised under Zone 4. The four zones were spatially illustrated in Fig. 4b, which showed that the sites proximate to Ras-Laffan industrial city, in front of Halul Island, and the majority of Qatari's oil fields were the sites under zone 1. Zone 2 represented the sites close to Dukhan city, while sites under zones 3 and 4 are mainly nearby the begets oil fields of Qatar (Al-Shaheen, Al-Rayyan oil fields) and close to the main shipping routes of the Arabian Gulf.

3.1. Total mercury analysis in tar-sediment samples

Table 7 displays the mean concentration of THg from the current study in the tarmat-sediment mixture and the THg in asphalt, crude oil, oil sludge, gasoline and diesel oil, and sediment samples from comparable studies. The overall average concentration of THg in the current study is $89 \pm 20 \text{ ng}\cdot\text{g}^{-1}$.

The results showed significant differences ($p \leq 0.05$) between north, northeast, east and west of Qatari coasts (Fig. 5). THg concentration was relatively higher only in three sites located in the north-northeast shoreline: Al Ghariya, $463 \pm 21 \text{ ng}\cdot\text{g}^{-1}$; Umm Al Far South, 445 ± 2

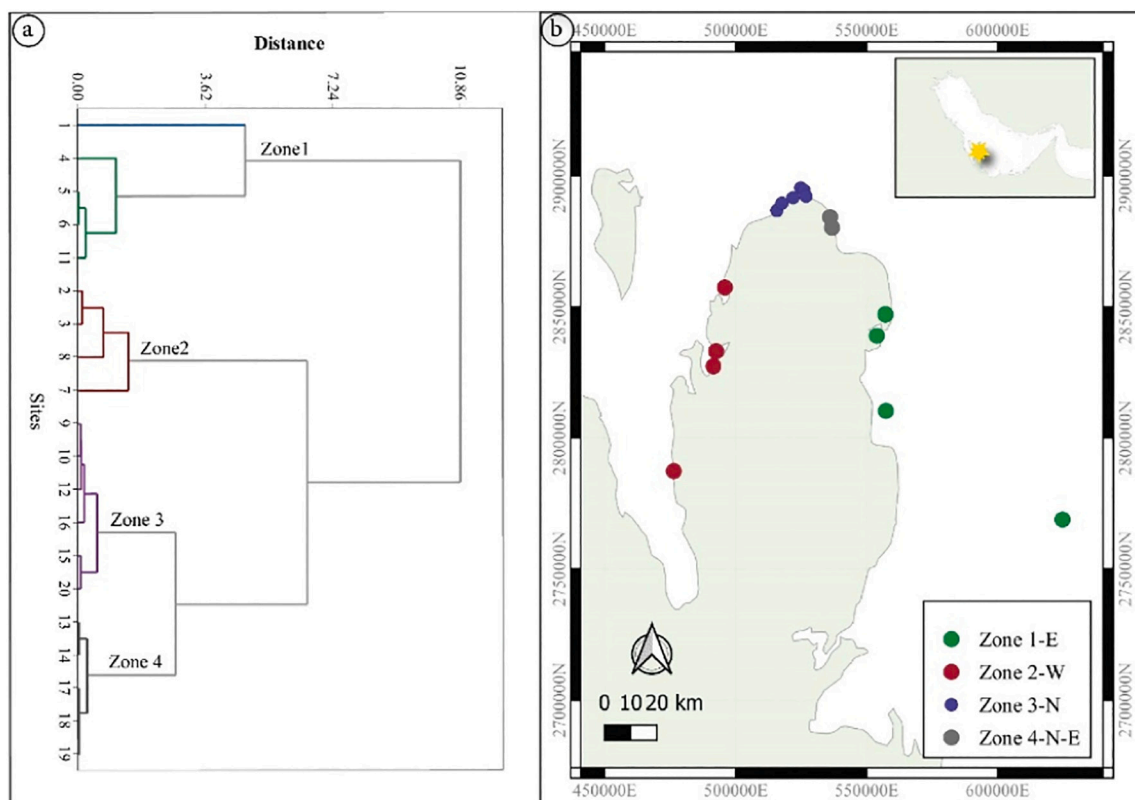


Fig. 4. Ward Linkage Euclidean distance (a) dendrogram and (b) particular representation of sampling sites.

Table 7

Total mercury ($\text{ng}\cdot\text{g}^{-1}$) in, asphalt, crude oils, oil sludge, gasoline, diesel oil, marine sediment, and tarmat-sediment mixture from different countries.

No.	Country	Sample type	THg ($\text{ng}\cdot\text{g}^{-1}$)	Ref
1	USA	Asphalt	0.27 ± 0.32	(Bloom, 2000)
2	Brazil	Crude oils 2	204 ± 11	(Pontes et al., 2013)
		Crude oils 3	46 ± 4	
		Oil sludge	443 ± 7	
3	USA	29 crude oil residues	220 ± 20 – 6440 ± 240	(May and Presley, 1975)
4	China	Gasoline and diesel oil	13–1250	(Yun et al., 2013)
5	Middle East	Crude oil	≤ 15	(IPIECA, 2014)
6	Indian and Pacific Ocean countries	Crude oil	> 100	
7	Qatar	Marine sediment	0.7–16.7	(de Mora et al., 2004)
8	Qatar	Marine sediment	8–34	(Hassan et al., 2019)
9	Qatar	Tarmat-sediment mixture	17 ± 10 – 460 ± 20	Current study

$\text{ng}\cdot\text{g}^{-1}$; and Fuwairit, $305 \pm 28 \text{ ng}\cdot\text{g}^{-1}$, while in other locations, the concentrations were less than $70 \text{ ng}\cdot\text{g}^{-1}$ (refer to Fig. 5). The THg concentrations in the samples of tarmat-sediment mixture in the present study is higher compared to the asphalt sample in the study of Bloom (2000) with a mean concentration of $0.27 \pm 0.32 \text{ ng}\cdot\text{g}^{-1}$ (Bloom, 2000). However, the THg levels in the present study were comparable to the THg concentration in the crude oils (2 and 3) and oil sludge residues from Brazil which obtained $204 \pm 11 \text{ ng}\cdot\text{g}^{-1}$, $46 \pm 4 \text{ ng}\cdot\text{g}^{-1}$, and $443 \pm 7 \text{ ng}\cdot\text{g}^{-1}$ respectively (Pontes et al., 2013). For crude oil from Texas, USA, the present results are in the lower end compared to the 29 crude oil residues analyzed which ranged from 220 ± 20 to $6440 \pm 240 \text{ ng}\cdot\text{g}^{-1}$ (May and Presley, 1975) and in the gasoline and diesel oil samples from China that had THg concentration that ranged from 13 to $1250 \text{ ng}\cdot\text{g}^{-1}$ (Yun et al., 2013). It is evident that mercury concentrations in crude oil vary depending on geographical source (refer to Table 9). Middle East crude oil was found to have levels that do not exceed $15 \text{ ng}\cdot\text{g}^{-1}$ while countries in Indian and Pacific Ocean have levels above $100 \text{ ng}\cdot\text{g}^{-1}$ (IPIECA, 2014). Canadian crude oil has THg concentration of $2.6 \pm 0.5 \text{ ng}\cdot\text{g}^{-1}$ (Hollebone and Yang, 2007). Hassan et al. (2019) recent study described the level of THg present in the Arabian Gulf sediments. Their

estimated values for THg concentration in the sediments ranged from 8 to $34 \text{ ng}\cdot\text{g}^{-1}$, which was relatively higher compared to the values estimated by de Mora et al. (2004) that ranged from 0.3 to $16.7 \text{ ng}\cdot\text{g}^{-1}$ in the nearshore sediments with the highest recorded level of $16.7 \text{ ng}\cdot\text{g}^{-1}$ near the northeast coastline of Ras Al Nouf. In comparison with the present study, we find a relatively higher concentration of THg ($463 \text{ ng}\cdot\text{g}^{-1}$) at the northeast coast (Fig. 5) which could be influenced by the presence of tarmats within the area which may be a result from the accumulated oil spill from the petroleum rig operations which are mostly found in the northeastern part of Qatar (refer to Fig. 2) and the fact that the Arabian gulf through the Strait of Hormuz is the busiest and most important oil transit chokepoint that is the route for large quantities of petroleum oil and products (Barden, 2019). However, the overall results indicated a significant drop in THg from the values reported (48000 – $250,000 \text{ ng}\cdot\text{g}^{-1}$) by Al-Majed and Rajab (1998) for the ROPME Sea Area after the 1991 Gulf War.

A significant variation ($p < 0.05$) in THg levels ($\text{ng}\cdot\text{g}^{-1}$) was observed between the North and East from one side and the West of Qatar from the other side (Table 8).

Fig. 6 confirm the variation in THg concentrations between the Qatar directions in favour of the North and East that may be due to the seepage and spills from the oil and gas extractions from the 11 oilfield operations across the coastline in addition to the wastewater effluent from the 3 adjacent industrial cities within the sampling areas (refer to Fig. 2). Oil refining is considered one of the major anthropogenic sources of mercury owing to the mass production and consumption of petroleum products which accounts for an estimated 0.65% of the global Hg input (Mojammal et al., 2019; United Nations Environment Programme (UNEP), 2019). Hydrodynamic circulation, tar and sedimentary depositional process may be the contributing factors that controlled the fate and distribution of Hg concentration in the study area.

Table 8

Post hoc test (Tukey HSD) for THg ($\text{ng}\cdot\text{g}^{-1}$) by four zones (Zone-1-E, Zone-2-W, Zone-3-N, and Zone-4-N-E).

Zone	Mean difference	Std. Error	P.Value	
Zone-4-N-E	Zone-1-E	94.56*	31.82	0.019
	Zone-2-W	137.86*	36.75	0.002
	Zone-3-N	134.21*	30.27	0.001

* The mean difference is significant at the 0.05 level.

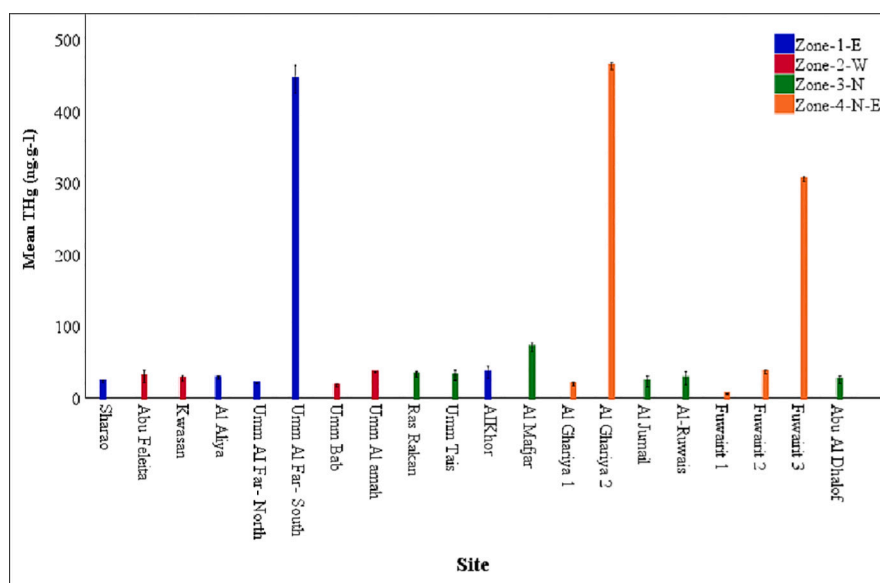


Fig. 5. The concentration of total mercury ($\text{ng}\cdot\text{g}^{-1}$) in the tarmat-sediments mixture obtained along the coast of Qatar.

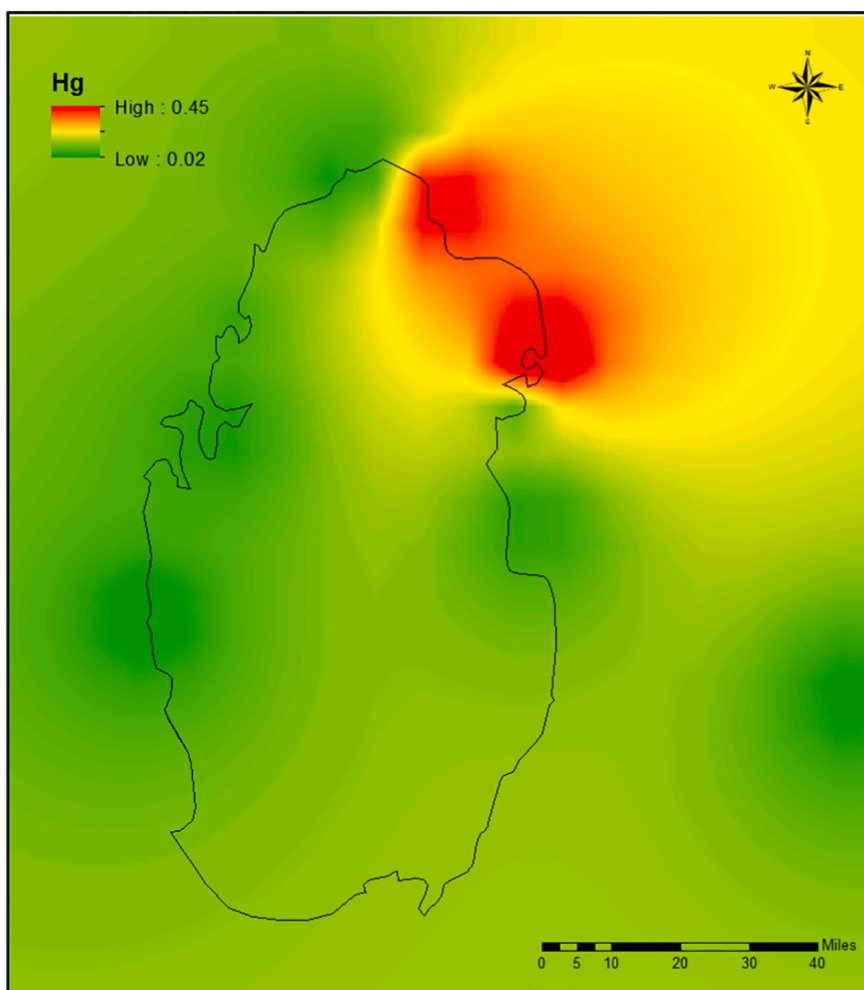


Fig. 6. Distribution of total mercury (T-Hg) measured along the Qatar coast.

3.2. THg analysis in biota samples

Biota species belonging to four families were found on the tarmats in Ras Rakan, Umm Tais, and Al-Mafjar. These species were analyzed for THg (Table 9). THg pollutants may directly affect organisms by accumulating in their body via ingestion routes or indirectly by transferring to the food chains through the higher trophic level (Shah, 2005). Hg bioaccumulation is influenced by size (Chouvelon et al., 2019; Cossa et al., 2012); differences in trophic level (Chen et al., 2014) tissue sample (Barrento et al., 2009; Harding et al., 2018), feeding habit (Chouvelon et al., 2019), sex of the organism, and sampling season (Barrento et al., 2009). Since there were not enough common species of

Table 9

Mean concentration of THg ($\text{ng}\cdot\text{g}^{-1}$), in seven biota species located in three tarmat sampling locations.

Class				THg ($\text{ng}\cdot\text{g}^{-1}$)	
				Mean	St-Dev
Gastropoda	<i>Cerithidea cingulata</i>	Al Mafjar	151	7	
		Ras Rakan	251	<1	
Bivalvia	<i>Asaphis</i> sp.	Ras Rakan	229	9	
		Umm Tais	729	16	
Crustacea (crab)	<i>Clibanarius signatus</i>	Ras Rakan	977	7	
		Umm Tais	116	2	
	<i>Leptodiis exaratus</i>	Umm Tais	144	<1	
		Ras Rakan	158	<1	

organisms found in the three study areas therefore it is impossible to perform a relevant pairwise comparison of THg accumulation in these locations (refer to Table 9). However, to evaluate the THg concentration in the muscle tissue of the obtained biota samples, ANOVA analysis was performed across all species in all locations. Significant differences were found in the THg accumulation in all biota samples ($p < 0.05$). The highest concentration of THg was found in the crustaceans' bodies, particularly the hermit crabs *Clibanarius signatus* with concentrations equal to $977 \pm 7 \text{ ng}\cdot\text{g}^{-1}$ followed by Bivalvia, while Gastropoda species represented minimal concentrations (Table 9). These classes are known for their accumulator strength, and it is believed to act as an important vector for 'pumping' Hg to higher trophic levels (Chen et al., 2014; Chouvelon et al., 2019; Gagnon and Fisher, 1997; Wang and Wang, 2010). The maximum oral dose for Hg consumption set by FDA (2020), and EPA (2019) is $\leq 460 \text{ ng}\cdot\text{g}^{-1}$ per week serving and the analyzed samples of marine bivalve, *Barabatia* cf. *setigera* in Umm Tais and the crustacea, *Clibanarius signatus* in Ras Rakan exceeded this limit.

Pearson correlation was also performed between groups of THg levels in biota and tarmat-sediment mixture samples. No significant correlation was detected in THg between biota and tarmat-sediment samples across all locations ($p > 0.05$). There is a common class of organisms belonging to crustacea observed in Umm Tais and Ras Rakan (refer to Table 9). Independent T-test was analyzed for this class. Significant differences were obtained between the crustaceans found with higher concentration in Ras Rakan than in Umm Tais ($p < 0.05$). The Pearson correlation analysis showed significant negative correlation between THg in the sampled crustaceans and the tarmat-sediment

samples from Ras Rakan and Umm Tais. ($p < 0.05$). The decrease in the Hg uptake in the sampled crustaceans may have been influenced by the higher salinity in the marine waters of Qatar (Curtis et al., 2019; Wang and Wang, 2010). Wang and Wang (2010) also found an inverse relationship between salinity and Hg uptake in certain marine organisms i.e. tilapia, *Oreochromis niloticus* in the presence of dissolved organic carbon. Inorganic Hg uptake rates dramatically decreased with higher salinity. The open gulf waters northeast of Qatar have salinities in the range of 40–42 psu (Rivers et al., 2019). This high salinity and the organic carbon present in the tar residues may have controlled the Hg bioaccumulation in crustacean samples. The bioavailability of sediment-bound Hg for organisms has a strong association with MeHg and other key geochemical parameters e.g. organic matter, iron, salinity (Gagnon and Fisher, 1997; Hammerschmidt and Fitzgerald, 2006; Pan and Wang, 2004; Cossa et al., 2012; Wang and Wang, 2010). The bioavailability of mercury both inorganic Hg and organic MeHg is highly controlled by the distribution of dissolved chemical complexes and physicochemical parameters of water and sediment due to the specific uptake mechanisms of different organisms (Curtis et al., 2019; Wang and Wang, 2010). Further study is recommended to evaluate Hg including MeHg uptake (and elimination) and certain physicochemical parameters in various common marine species and their habitats.

3.3. Ecological risk assessment

High concentrations of mercury pose several issues to the environment and to refineries. According to the sediment quality guideline of National Oceanic and Atmospheric Administration (NOAA), the Threshold Effects Level (TEL) and the Probable Effects Level (PEL) for THg is $130 \text{ ng}\cdot\text{g}^{-1}$ and $700 \text{ ng}\cdot\text{g}^{-1}$ respectively (Buchman, 2008). Based on the results of this study, only samples from Al Ghariya ($463 \pm 21 \text{ ng}\cdot\text{g}^{-1}$); Umm Al Far South ($445 \pm 2 \text{ ng}\cdot\text{g}^{-1}$); and Fuwairit ($305 \pm 28 \text{ ng}\cdot\text{g}^{-1}$) exceeded the TEL limit.

Based on potential ecological risk index (E_r), the results indicated contamination factor (C_f) of Hg in a tarmat-sediment mixture ranging from low to considerable very high (0.145–13.57) with an average value of 1.82 (moderate contamination). Compared to the previous studies, the mean contamination factor of Hg in the present study is considered higher than that measured in Al-Jubail area, Arabian Gulf (El-Sorogy et al., 2018) and that in the northern coasts of the Gulf of Oman (Abkenar et al., 2021). The contamination factor of Hg in sediments in the Arabian Gulf (Persian Gulf) was consistent with the current results (1.10–2.22) (Ranjbar Jafarabadi et al., 2017). However, the mean (C_f) of Hg evaluated recently in Iran was very high (8.12) compared with the current study, which was attributed to anthropogenic activities (Elsagh et al., 2021). The potential ecological risk index (E_r) represented low to serious ecological risk ranging 5.8–543 with an average value of 72.9. There were three sites in descending order: Al Ghariya-2 > Umm Al Far-South > Fuwairit-3 with serious ecological hazards of 539.5, 518.1, 355.7 respectively and 1 site (Al-Mafjar) with higher ecological hazards (82.7). In the other sites (E_r) were fluctuated from moderate to low. The mean calculated value of E_r , was taken to understand the potential ecological risk index within each zone, and characterized as High, Higher, Moderate, and Low risk in Zone 4 > Zone 1 > Zone 3 > Zone 2, respectively.

3.4. Pollution load index (PLI)

There were three highly polluted sites: Al Ghariya-2 > Umm Al Far-South > Fuwairit-3 with PLI values of 13.49, 12.95, 8.89 respectively and one site moderately polluted (2.07) at Al-Mafjar. In the other sites, PLI were fluctuating from no pollution to moderate pollution. The pollution load index (PLI) was calculated for each zone and the highest PLI value was obtained from zone 4 (2.09) representing moderate pollution, followed by zone 1 (1.34) indicating slight pollution, while zone 3, 2 (<1) representing no pollution. Thus, the descending order of

PLI within the four clustered zones was Zone 4 > Zone 1 > Zone 3 > Zone 2. The highest PLI of the current study (2.09) is low compared with that obtained in sediment in the Arabian Gulf (Persian Gulf) ranging 2.19–5.86 and in China with an average value of 4.40 (Ranjbar Jafarabadi et al., 2017; Shi et al., 2020).

3.5. Geoaccumulation index (I_{geo})

The geoaccumulation index (I_{geo}) was evaluated for each site using Eq. (4), with mean value of 0.93. The max values of 4.49, 4.43, 3.89 were found in Al Ghariya, Umm Al Far, and Fuwairit, respectively as moderately to strongly polluted sites. In contrast, other sites were characterized as unpolluted to moderately polluted sites ranging from 0.0 to 1.79. The mean values of I_{geo} within each Zone were obtained and characterized. I_{geo} in Zone 4 (1.45), followed by zone 1 (1.16), representing unpolluted to moderately polluted. In contrast, zone 3, 2 (<1) indicate unpolluted zone with descending order as Zone 4 > Zone 1 > Zone 3 > Zone 2. The current mean values were low compared to the previous studies (1.87–2.11) in the Arabian Gulf (El-Sorogy et al., 2018; Elsagh et al., 2021).

3.6. Toxic risk index (TRI)

Toxic risk index (TRI) of tarmat-sediment samples were applied to evaluate the Hg pollution caused by natural and anthropogenic activities along the Qatari coast. The mean values of the TRI in Hg were calculated using Eq. (5), and the results ranged from 1.0 to 5.18, with a mean of 3.41 indicating no toxic risk (Ranjbar Jafarabadi et al., 2017); however, the low toxic risk was observed at the north of Qatar (Zone 3). The current mean value of TRI was low compared to the previous studies in the Arabian Gulf which ranged from 5.23 to 17.92 (Elsagh et al., 2021; Ranjbar Jafarabadi et al., 2017).

3.7. Biota sediment accumulation factor (BSAF)

Biota sediment accumulation factor (BSAF) was calculated according to Eq. (6), and the results were shown in Table 10.

It shows BSAF results of THg that is >2 in all species. The organism can be classified as macro-concentrators. Macro-concentrators could be remarkably suggested as an appropriate biomonitoring object (Bohac, 1999). Ziyaadini et al. (2016) studied the BSAF of Hg and heavy metals in Iran, and the results ranging from 0.71–1.21. An earlier study assessed the biota sediment accumulation factor of total mercury and other metals in two marine bivalves, and it found the BSAF of Hg was approximately 1 (Thomann et al., 1995). A recent study measured BSAF of the shore crab tissues and sediment at Mousa Bay located in the north of the Arabian Gulf and the obtained range was between 0.4 and 1.14 (Saadati et al., 2020). In the current study, the detected BSAF of mercury levels was mostly elevated in crab and bivalvia species, especially *Clibanarius signatus* and *Barbatia setigera*. The presence of the levels of THg

Table 10

Biota sediment accumulation factor (BSAF) of THg in seven species collected from three locations in the north of Qatar coastline.

Subphylum/species	Location	BSAF
Crustacea (crab)		
<i>Leptodius exaratus</i>	Umm Tais	4.38
<i>Metopograpsus messor</i>	Ras Rakan	4.85
Crustacea (hermit crab)		
<i>Clibanarius signatus</i>	Ras Rakan	29.70
<i>Clibanarius signatus</i>	Umm Tais	3.75
Mollusca (Bivalvia)		
<i>Asaphis</i> sp.	Ras Rakan	6.97
<i>Barbatia setigera</i>	Umm Tais	22.81
Mollusca (Gastropoda)		
<i>Lunella coronata</i>	Ras Rakan	7.58
<i>Pirenella cingulata</i>	Al Mafjar	2.11

in the soft tissues of these species could be caused by their role as carriers of metabolically important biomolecules including enzymes, metalloenzymes, and respiratory pigments, and indicates that the source of uptake is ingestion from their habitat i.e. tar/sediments media as suggested by Förstner and Prosi (1979). In this study, the comparison of different organisms provided evidence on good biomonitors, however the organisms bioaccumulation capacity is species-specific and metal-specific. The maximum obtained BSAF in the present study was 29.70, and is obtained from *Clibanarius signatus*, followed by *Barbatia setigera* species with values 22.81 (Table 10).

The BSAF in in Crustacea (crab) sp. Crabs and bivalves are found as adequate biomonitors for metal contaminants in marine environments although bivalves are most frequently used in most studies (Li et al., 2019). These species may become vectors of transport of THg pollutant in the marine food chain. Similar results on the species-specific bioaccumulation of metals from the environment, that results from many factors such as diet, physiological activities and metabolic abilities of organisms and metal concentrations in the habitat and food have been previously reported (Li et al., 2019). Biomonitoring has become a well-accepted and adopted scientific technique for environmental exposure assessment which the organisms' high tolerance to pollution, high accumulation capacity, wide distribution, easy identification and limited mobility are suitable criteria for an organism to be a perfect biomonitor (Li et al., 2019).

4. Conclusions

Tarmat is an environmental issue along the Qatar coast, particularly in the eco-sensitive regions. Though oil spills can be removed, and beaches cleaned, it is rather difficult to remove the residue they left behind; in fact, tarmat is far more threatening than the original spill. It is the accumulation of years of small spill residues. Although there is a conscience that most of the contaminants on the surface of the tarmats have long past evaporated to insignificant levels due to weathering factors, the fact remains that some pollutants have persisted within them. The present study has shown level of THg pollutant in the tarmat-sediment samples, with moderate to serious potential ecological risk index, and moderate pollution load index especially in Qatar's north and northeast shorelines due to the direct exposure to transport of oil spills, the country's coastal topography, geomorphology and hydrodynamic circulation. Other sites observed low THg concentrations which may be due highly weathered tarmats that looked like asphalt indicative of a solidified old oil spill which were likely from the three-decade old oil spill of 1991 Gulf War.

Compared to previous studies done on the asphalt, crude oil and marine sediment, the present study reports higher levels of Hg to a number of sites. Therefore, it needs to be ascertained whether this increase results from tarmat, sampling locations, or other factors. As Qatar's exclusive economic zone is experiencing rapid industrial and urban development, it is prudent to monitor all contaminants having the potential of bioaccumulation and investigate their sources. Hg concentrations related to industrial emissions is further recommended to evaluate the atmospheric deposition of Hg in the country.

Funding

This work was supported by Qatar Petroleum through Qatar University, grant No. QUEx-ESC-QP-TM-18/19-01. The authors are responsible for the views expressed in this article.

CRediT authorship contribution statement

Ahmed About Elezz: Conceptualization, Methodology, Validation, Writing – original draft, Writing – review & editing. **Azenith Castillo:** Methodology, Data curation, Writing – original draft, Writing – review & editing. **Hassan Mustafa Hassan:** Validation, Investigation, Data

curation, Writing – review & editing, Visualization. **Hamood Abdulla Alsaadi:** Formal analysis, Validation. **Ponnumony Vethamony:** Supervision, Project administration.

Declaration of competing interest

The authors declare that they have no known competing financial interests or personal relationships that could have appeared to influence the work reported in this paper.

Acknowledgments

The authors thank Prof. Hamad Al-Kuwari, Director of the ESC, for his providing all facilities to carry out this work. We acknowledge the help of Mrs. Hajer Alnaimi (Technical Manager) provided while conducting the experiments. Special thanks to the ESC sampling team for their assistance.

References

- Abkenar, A.M., Yahyavi, M., Esmaeili, M., Rombenso, A., 2021. High bioaccumulation factors and ecological risk index of Cd and Hg in Indian white shrimp, hooded oyster, brown algae, and sediment in northern coasts of the Gulf of Oman before and after a monsoon. *Reg. Stud. Mar. Sci.* 41, 101552 <https://doi.org/10.1016/j.rsma.2020.101552>.
- Al-Kaabi, N.S., Kristensen, M., Zouari, N., Solling, T.I., Bach, S.S., Al-Ghouthi, M., Christensen, J.H., 2017. Source identification of beached oil at Al Zubarah, northwestern Qatar. *J. Pet. Sci. Eng.* 149, 107–113. <https://doi.org/10.1016/j.petrol.2016.10.034>.
- Al-Majed, N., Rajab, W.A., 1998. Levels of mercury in the marine environment of the ROPME sea area. In: Otsaki, A., Abdulraheem, M.Y., Reynolds, R.M. (Eds.), *Terra ScientiOffshore Environment of the ROPME Sea Area after the War-Related Oil Spills*, pp. 124–147.
- Angulo, E., 1996. The tomlinson pollution load index applied to heavy metal, "mussel-watch" data: a useful index to assess coastal pollution. *Sci. Total Environ.* 187, 19–56. [https://doi.org/10.1016/0048-9697\(96\)05128-5](https://doi.org/10.1016/0048-9697(96)05128-5).
- Arekhi, M., Terry, L.G., John, G.F., Al-Khayat, J.A., Castillo, A.B., Vethamony, P., Clement, T.P., 2020. Field and laboratory investigation of tarmat deposits found on Ras Rakan Island and northern beaches of Qatar. *Sci. Total Environ.* 735, 139516 <https://doi.org/10.1016/j.scitotenv.2020.139516>.
- Bailey, E.H., Snavely Jr., P.D., DEW, 1961. Chemical analyses of brines and crude oil, Cymric Field, Kern County, California. In: *Short Papers in the Geologic and Hydrologic Sciences*. U.S. Government Printing Office, pp. 306–309. <https://doi.org/10.3133/PP424D>.
- Barden, J., 2019. The Strait of Hormuz Is the World's Most Important Oil Transit Chokepoint. *Today in Energy*, 20.
- Barrento, S., Marques, A., Teixeira, B., Carvalho, M.L., Vaz-Pires, P., Nunes, M.L., 2009. Influence of season and sex on the contents of minerals and trace elements in Brown crab (*Cancer pagurus*, Linnaeus, 1758). *J. Agric. Food Chem.* 57, 3253–3260. <https://doi.org/10.1021/jf8039022>.
- Bejarano, A.C., Michel, J., 2010. Large-scale risk assessment of polycyclic aromatic hydrocarbons in shoreline sediments from Saudi Arabia: environmental legacy after twelve years of the Gulf war oil spill. *Environ. Pollut.* 158, 1561–1569. <https://doi.org/10.1016/j.envpol.2009.12.019>.
- Bloom, N.S., 2000. Analysis and stability of mercury speciation in petroleum hydrocarbons. *Fresenius J. Anal. Chem.* 366, 438–443. <https://doi.org/10.1007/s002160050089>.
- Bohac, J., 1999. Staphylinid beetles as bioindicators. In: *Invertebrate Biodiversity as Bioindicators of Sustainable Landscapes*. Elsevier, pp. 357–372. <https://doi.org/10.1016/b978-0-444-50019-9.50020-0>.
- Buchman, M.F., 2008. *Screening Quick Reference Tables (SQUIRTs)*.
- Burns, K.A., Villeneuve, J.P., Anderlin, V.C., Fowler, S.W., 1982. Survey of tar, hydrocarbon and metal pollution in the coastal waters of Oman. *Mar. Pollut. Bull.* 13, 240–247. [https://doi.org/10.1016/0025-326X\(82\)90347-2](https://doi.org/10.1016/0025-326X(82)90347-2).
- Chen, C.Y., Borsuk, M.E., Bugge, D.M., Hollweg, T., Balcom, P.H., Ward, D.M., Williams, J., Mason, R.P., 2014. Benthic and pelagic pathways of methylmercury bioaccumulation in estuarine food webs of the Northeast United States. *PLoS One* 9, e89305. <https://doi.org/10.1371/journal.pone.0089305>.
- Chouvelon, T., Strady, E., Harmelin-Vivien, M., Radakovitch, O., Brach-Papa, C., Crochet, S., Knoery, J., Rozuel, E., Thomas, B., Tronczynski, J., Chiffolleau, J.F., 2019. Patterns of trace metal bioaccumulation and trophic transfer in a phytoplankton-zooplankton-small pelagic fish marine food web. *Mar. Pollut. Bull.* 146, 1013–1030. <https://doi.org/10.1016/j.marpolbul.2019.07.047>.
- Coles, S.L., Gunay, N., 1989. Tar pollution on Saudi Arabian Gulf beaches. *Mar. Pollut. Bull.* 20, 214–218. [https://doi.org/10.1016/0025-326X\(89\)90433-5](https://doi.org/10.1016/0025-326X(89)90433-5).
- Cossa, D., Harmelin-Vivien, M., Mellon-Duval, C., Loizeau, V., Averty, B., Crochet, S., Chou, L., Cadiou, J.-F., 2012. Influences of bioavailability, trophic position, and growth on methylmercury in hakes (*Merluccius merluccius*) from northwestern Mediterranean and northeastern Atlantic. *Environ. Sci. Technol.* 46, 4885–4893. <https://doi.org/10.1021/es204269w>.

- Curtis, A., Bourne, K., Borsuk, M., Buckman, K., Demidenko, A., Taylor, V., Chen, C., 2019. Effects of temperature, salinity, and sediment organic carbon on methylmercury bioaccumulation in an estuarine amphipod. *Sci. Total Environ.* 687 <https://doi.org/10.1016/j.scitotenv.2019.06.094>. Effects, 907–016.
- Dahab, Ossama Aboul, 1994. *State of Oil Pollution Along the Qatari Coastline*.
- Dash, S., Borah, S.S., Kalamdhad, A.S., 2021. Heavy metal pollution and potential ecological risk assessment for surficial sediments of Deepor Beel, India. *Ecol. Indic.* 122, 107265. <https://doi.org/10.1016/j.ecolind.2020.107265>.
- de Jesus, A., Zmozinski, A.V., Vieira, M.A., Ribeiro, A.S., da Silva, M.M., 2013. Determination of mercury in naphtha and petroleum condensate by photochemical vapor generation atomic absorption spectrometry. *Microchem. J.* 110, 227–232. <https://doi.org/10.1016/j.microc.2013.03.019>.
- de Mora, S., Fowler, S.W., Wyse, E., Azemard, S., 2004. Distribution of heavy metals in marine bivalves, fish and coastal sediments in the Gulf and Gulf of Oman. *Mar. Pollut. Bull.* 49, 410–424. <https://doi.org/10.1016/j.marpolbul.2004.02.029>.
- Dhamodharan, A., Abinandan, S., Aravind, U., Ganapathy, G.P., Shanthakumar, S., 2019. Distribution of metal contamination and risk indices assessment of surface sediments from Cooum River Chennai India. *Int. J. Environ. Res.* 13, 853–860. <https://doi.org/10.1007/s41742-019-00222-8>.
- ECHA, 2012. *Guidance on information requirements and chemical safety assessment*. In: Chapter R. 14: Occupational exposure estimation.
- Elezz, A., Mustafa Hassan, H., Abdulla Alsaadi, H., Easa, A., Al-Meer, S., Elsaid, K., Ghouri, Z., Abdala, A., 2018. Validation of Total mercury in marine sediment and biological samples, using cold vapour atomic absorption spectrometry. *Methods Protoc.* 1, 31. <https://doi.org/10.3390/mps1030031>.
- Elsagh, A., Jalilian, H., Ghaderi Alishabestari, M., 2021. Evaluation of heavy metal pollution in coastal sediments of Bandar Abbas, the Persian Gulf, Iran: mercury pollution and environmental geochemical indices. *Mar. Pollut. Bull.* 167, 112314 <https://doi.org/10.1016/j.marpolbul.2021.112314>.
- El-Sorogy, A., Al-Kahtany, K., Youssef, M., Al-Kahtany, F., Al-Malky, M., 2018. Distribution and metal contamination in the coastal sediments of Dammam Al-Jubail area, Arabian Gulf, Saudi Arabia. *Mar. Pollut. Bull.* 128, 8–16. <https://doi.org/10.1016/j.marpolbul.2017.12.066>.
- EPA, U., 2019. EPA-FDA advice about eating fish and shellfish. In: *Advisories and Technical Resources for Fish and Shellfish Consumption*. US EPA [WWW Document].
- Farooqui, N.U., Al Zahrani, D.A., El Selim, M.M., Dangi, C.B.S., 2015. A review on the impact of exotoxicology and oil spills in mangrove of Saudi Arabia. *J. Pure Appl. Microbiol.* 9, 549–556.
- FDA, 2020. *Technical Information on Development of FDA/EPA Advice about Eating Fish for Those Who Might Become or Are Pregnant or Breastfeeding and Children Ages 1-11 Years* [WWW Document]. Food Drug Adm. <https://www.fda.gov/food/metals-and-your-food/technical-information-development-fdaepa-advice-about-eating-fish-those-who-might-become-or-are> (accessed 11.17.21).
- Förstner, U., Prosi, F., 1979. Heavy metal pollution in freshwater ecosystems. In: *Biological Aspects of Freshwater Pollution*. Elsevier, pp. 129–161. <https://doi.org/10.1016/B978-0-08-023442-7.50011-6>.
- Fowler, S.W., 1985. Coastal baseline studies of pollutants in Bahrain, UAE and Oman. In: *Proceedings of a Regional Symposium for the Evaluation of Marine Pollution Monitoring and Research Programmes*. Al Ain, UAE, pp. 155–180.
- Freije, A.M., 2015. Heavy metal, trace element and petroleum hydrocarbon pollution in the Arabian Gulf. review. *J. Assoc. Arab Univ. Basic Appl. Sci.* 17, 90–100. <https://doi.org/10.1016/j.jaubas.2014.02.001>.
- Freije, A., Awadh, M., 2009. Total and methyl mercury intake associated with fish consumption in Bahrain. *Water Environ. J.* 23, 155–164. <https://doi.org/10.1111/j.1747-6593.2008.00129.x>.
- Gagnon, C., Fisher, N.S., 1997. Bioavailability of sediment-bound methyl and inorganic mercury to a marine bivalve. *Environ. Sci. Technol.* 31, 993–998. <https://doi.org/10.1021/es960364k>.
- Ghosn, M., Mahfouz, C., Chekri, R., Ouddane, B., Khalaf, G., Guérin, T., Amara, R., Jitaru, P., 2020. Assessment of trace element contamination and bioaccumulation in algae (*Ulva lactuca*), bivalves (*Spondylus spinosus*) and shrimps (*Marsupenaeus japonicus*) from the Lebanese coast. *Reg. Stud. Mar. Sci.* 39, 101478 <https://doi.org/10.1016/j.rsm.2020.101478>.
- Goodman, R., 2003. Tar balls: the end state. *Spill Sci. Technol. Bull.* 8, 117–121. [https://doi.org/10.1016/S1353-2561\(03\)00045-8](https://doi.org/10.1016/S1353-2561(03)00045-8).
- Guo, W., Liu, X., Liu, Z., Li, G., 2010. Pollution and potential ecological risk evaluation of heavy metals in the sediments around Dongjiang Harbor, Tianjin. *Procedia Environ. Sci.* 2, 729–736. <https://doi.org/10.1016/j.proenv.2010.10.084>.
- Hammerschmidt, C.R., Fitzgerald, W.F., 2006. Methylmercury cycling in sediments on the continental shelf of southern New England. *Geochim. Cosmochim. Acta* 70, 918–930. <https://doi.org/10.1016/j.gca.2005.10.020>.
- Harding, G., Dalziel, J., Vass, P., 2018. Bioaccumulation of methylmercury within the marine food web of the outer Bay of Fundy, Gulf of Maine. *PLoS One* 13, e0197220. <https://doi.org/10.1371/journal.pone.0197220>.
- Hassan, H., Elezz, A.A., Abuasali, M., Alsaadi, H., 2019. Baseline concentrations of mercury species within sediments from Qatar's coastal marine zone. *Mar. Pollut. Bull.* 142, 595–602. <https://doi.org/10.1016/j.marpolbul.2019.04.022>.
- Hayworth, J.S., Clement, T.P., 2011. BP's operation deep clean—could dilution be the solution to beach pollution? *Environ. Sci. Technol.* 45, 4201–4202. <https://doi.org/10.1021/es201242k>.
- Hoff, R., Hensel, P., Yender, R., Mearns, A.J., Michel, J., Proffitt, E.C., Shigenaka, G., Hoff, R., Michel, J., Michel, J., Delgado, P., 2014. *Oil Spills in Mangroves: Planning & Response Considerations*. NOAA (accessed 11.17.21).
- Hollebone, B.P., Yang, C.X., 2007. Mercury in crude oil refined in Canada. *Environ. Can.* 1–82.
- IPIECA, 2014. *Mercury management in petroleum refining*, 36.
- Islam, M.S., Ahmed, M.K., Raknuzzaman, M., Islam, M.K., Habibullah-Al-Mamun, M., 2015. Heavy metal pollution in surface water and sediment: A preliminary assessment of an urban river in a developing country. *Ecol. Indic.* 48, 282–291. <https://doi.org/10.1016/j.ecolind.2014.08.016>.
- Kruger, M.A., Lara-Gonzalo, A., Gallego, J.L.R., 2020. Environmental forensics of complexly contaminated sites: a complimentary fingerprinting approach. *Environ. Pollut.* 263, 114645 <https://doi.org/10.1016/j.envpol.2020.114645>.
- Li, D., Wang, J., Pi, J., Yu, J., Zhang, T., 2019. Biota-sediment metal accumulation and human health risk assessment of freshwater bivalve *Corbicula fluminea* in Dongting Lake, China. *Environ. Sci. Pollut. Res.* 26, 14951–14961. <https://doi.org/10.1007/s11356-019-04931-7>.
- Liu, D., Ma, J., Sun, Y., Li, Y., 2016. Spatial distribution of soil magnetic susceptibility and correlation with heavy metal pollution in Kaifeng City, China. *Catena* 139, 53–60. <https://doi.org/10.1016/j.catena.2015.11.004>.
- Liu, R., Wang, M., Chen, W., Peng, C., 2016. Spatial pattern of heavy metals accumulation risk in urban soils of Beijing and its influencing factors. *Environ. Pollut.* 210, 174–181. <https://doi.org/10.1016/j.envpol.2015.11.044>.
- May, L.A., Presley, B.J., 1975. Mercury in crude oil residues. *Chemosphere* 4, 329–332. [https://doi.org/10.1016/0045-6535\(75\)90026-0](https://doi.org/10.1016/0045-6535(75)90026-0).
- Michel, J., Owens, E.H., Zengel, S., Graham, A., Nixon, Z., Allard, T., Holton, W., Reimer, P.D., Lamarche, A., White, M., Rutherford, N., Childs, C., Mauseth, G., Challenger, G., Taylor, E., 2013. Extent and degree of shoreline oiling: Deepwater horizon oil spill, Gulf of Mexico, USA. *PLoS One* 8, e65087. <https://doi.org/10.1371/journal.pone.0065087>.
- Mohamed, H.H.A., Mohamed, R.A.F., 2005. Accumulation of trace metals in some benthic invertebrate and fish species relevant to their concentration in water and sediment of Lake Qarun, Egypt. *Egypt. J. Aquat. Res.* 31, 289–301.
- Mojammal, A.H.M., Back, S.-K., Seo, Y.-C., Kim, J.-H., 2019. Mass balance and behavior of mercury in oil refinery facilities. <https://doi.org/10.1016/j.apr.2018.07.002>.
- Müller, G., 1969. Index of geoaccumulation in sediments of the Rhine River. *Geol. J.* 2, 108–118.
- NAS, 2003. *Oil in the Sea III*, The National Academies Press. National Academies Press, Washington, D.C. <https://doi.org/10.17226/10388>.
- Nenciu, M., Oros, A., Roşioru, D., Galatci, M., Filimon, A., Ţiganov, G., Danilov, C., Roşoiu, N., 2016. Heavy metal bioaccumulation in marine organisms from the Romanian Black Sea coast. *Ser. Biol. Sci.* 5, 38–52.
- Otuya, B.O., Akporohor, E.E., Achuba, F.I., 2008. Determination of heavy metals in toads exposed to oil polluted environment (Ekpan) Delta state, Nigeria. *Environmentalist* 28, 405–408. <https://doi.org/10.1007/s10669-007-9159-8>.
- Pan, J., Wang, W., 2004. Uptake of Hg(II) and methylmercury by the green mussel *Perna viridis* under different organic carbon conditions. *Mar. Ecol. Prog. Ser.* 276, 125–136. <https://doi.org/10.3354/meps276125>.
- Pandey, S.K., Kim, K.-H., Yim, U.-H., Jung, M.-C., Kang, C.-H., 2009. Airborne mercury pollution from a large oil spill accident on the west coast of Korea. *J. Hazard. Mater.* 164, 380–384. <https://doi.org/10.1016/j.jhazmat.2008.07.126>.
- Pérez-López, M., Cid, F., Oropesa, A.L., Fidalgo, L.E., Beceiro, Ana López, Soler, F., 2006. Heavy metal and arsenic content in seabirds affected by the prestige oil spill on the Galician coast (NW Spain). *Sci. Total Environ.* 359, 209–220. <https://doi.org/10.1016/j.scitotenv.2005.04.006>.
- Pontes, Fernanda Veronesi, M., Carneiro, M.C., Vaitsman, D.S., Monteiro, M.I.C., Neto, A. A., Tristão, M.L.B., Guerrante, M.D.F., 2013. Comparative study of sample decomposition methods for the determination of total Hg in crude oil and related products. *Fuel Process. Technol.* 106, 122–126. <https://doi.org/10.1016/j.fuproc.2012.07.011>.
- Qatar Petroleum, 2019. *Oil and Gas Fields* [WWW Document]. QP Website. <https://www.qp.com.qa/en/QPActivities/QPOperations/Pages/OilAndGasFields.aspx> (accessed 9.30.21).
- Rajendran, S., Al-Khayat, J.A., Veerasingam, S., Nasir, S., Vethamony, P., Sadooni, F.N., Al-Kuwari, H.A.-S., 2021. WorldView-3 mapping of tar mat deposits of the Ras Rakan Island, northern coast of Qatar: environmental perspective. *Mar. Pollut. Bull.* 163, 111988 <https://doi.org/10.1016/j.marpolbul.2021.111988>.
- Ranjbar Jafarabadi, A., Riyahi Bakhtiyari, A., Shadmehri Toosi, A., Jadot, C., 2017. Spatial distribution, ecological and health risk assessment of heavy metals in marine surface sediments and coastal seawaters of fringing coral reefs of the Persian Gulf, Iran. *Chemosphere* 185, 1090–1111. <https://doi.org/10.1016/j.chemosphere.2017.07.110>.
- Rivers, J.M., Varghese, L., Yousif, R., Whitaker, F.F., Skeat, S.L., Al-Shaikhi, I., 2019. The geochemistry of Qatar coastal waters and its impact on carbonate sediment chemistry and early marine diagenesis. *J. Sediment. Res.* 89, 293–309. <https://doi.org/10.2110/jsr.2019.17>.
- Rocha, J.E., Guedes, T.A.M., Bezerra, C.F., Campina, F.F., de Freitas, T.S., Souza, A.K., Sobral Souza, C.E., Silva, M.K.N.N., Lobo, Y.M., Pereira-Junior, F.N., da Silva, J.H., Menezes, I.R.A.A., Teixeira, R.N.P.P., Teixeira, A.M.R.R., Colares, A.V., Coutinho, H. D.M.M., Costa, M.do S., 2019. Mercury chloride phytotoxicity reduction using antioxidative mechanisms evidenced by caffeic acid FTIR. *Appl. Geochem.* 104, 109–115. <https://doi.org/10.1016/j.apgeochem.2019.03.015>.
- Saadati, M., Soleimani, M., Sadeghsaba, M., Hemami, M.R., 2020. Bioaccumulation of heavy metals (Hg, Cd and Ni) by sentinel crab (*Macrophthalmus depressus*) from sediments of Mousa Bay, Persian Gulf. *Ecotoxicol. Environ. Saf.* 191, 109986 <https://doi.org/10.1016/j.ecoenv.2019.109986>.
- Scanex, G.I.-R., 2018. *Satellite Monitoring of Oil Pollution in the Persian Gulf* — ScanEx [WWW Document]. Scanex. <http://www.scanex.ru/en/company/news/satellite-monitoring-of-oil-pollution-in-the-persian-gulf/> (accessed 6.19.20).
- Shah, S.-L., 2005. Effects of Heavy Metal Accumulation on the 96-h LC₅₀ Values in Tench *Tinca tinca* L., 1758. *Turk. Vat J. Anim. Sci.* 29, 139–144.

- Shi, C., Yu, L., Chai, M., Niu, Z., Li, R., 2020. The distribution and risk of mercury in Shenzhen mangroves, representative urban mangroves affected by human activities in China. *Mar. Pollut. Bull.* 151, 110866 <https://doi.org/10.1016/j.marpolbul.2019.110866>.
- Thomann, R.V., Mahony, J.D., Mueller, R., 1995. Steady-state model of biota sediment accumulation factor for metals in two marine bivalves. *Environ. Toxicol. Chem.* 14, 1989–1998. <https://doi.org/10.1002/etc.5620141121>.
- United Nations Environment Programme (UNEP), 2019. *Global Mercury Assessment 2018* [WWW Document]. UN Environ. Program. Chem. Heal. Branch, Geneva, Switz.
- Veerasingam, S., Al-Khayat, J.A., Haseeba, K.P., Aboobacker, V.M., Hamza, S., Vethamony, P., 2020. Spatial distribution, structural characterization and weathering of tarmats along the west coast of Qatar. *Mar. Pollut. Bull.* 159, 111486 <https://doi.org/10.1016/j.marpolbul.2020.111486>.
- Wang, R., Wang, W.X., 2010. Importance of speciation in understanding mercury bioaccumulation in tilapia controlled by salinity and dissolved organic matter. *Environ. Sci. Technol.* 44, 7964–7969. <https://doi.org/10.1021/es1011274>.
- Warnock, A.M., Hagen, S.C., Passeri, D.L., 2015. Marine tar residues: a review. *Water Air Soil Pollut.* 226, 68. <https://doi.org/10.1007/s11270-015-2298-5>.
- Wedepohl, K.K.T.K.H., 1961. Distribution of the elements in some major units of the Earth's crust. *GSA Bull.* 72, 175–192.
- Wilhelm, S.M., Bloom, N., 2000. Mercury in petroleum. *Fuel Process. Technol.* 63, 1–27. [https://doi.org/10.1016/S0378-3820\(99\)00068-5](https://doi.org/10.1016/S0378-3820(99)00068-5).
- Yun, Z., He, B., Wang, Z., Wang, T., Jiang, G., 2013. Evaluation of different extraction procedures for determination of organic mercury species in petroleum by high performance liquid chromatography coupled with cold vapor atomic fluorescence spectrometry. *Talanta* 106, 60–65. <https://doi.org/10.1016/j.talanta.2012.12.009>.
- Zhang, G., Bai, J., Zhao, Q., Lu, Q., Jia, J., Wen, X., 2016. Heavy metals in wetland soils along a wetland-forming chronosequence in the Yellow River Delta of China: levels, sources and toxic risks. *Ecol. Indic.* 69, 331–339. <https://doi.org/10.1016/j.ecolind.2016.04.042>.
- Zhao, J., Temimi, M., Al Azhar, M., Ghedira, H., 2015. Satellite-based tracking of oil pollution in the arabian gulf and the sea of Oman. *Can. J. Remote. Sens.* 41, 113–125. <https://doi.org/10.1080/07038992.2015.1042543>.
- Ziyaadini, M., Yousefyanpour, Z., Ghasemzadeh, J., Zahedi, M.M., 2016. Biota-sediment accumulation factor and concentration of heavy metals (Hg, Cd, As, Ni, Pb and Cu) in sediments and tissues of Chiton lamyi (Mollusca: Polyplacophora: Chitonidae) in Chabahar Bay, Iran. *Iran. J. Fish. Sci.* 16, 1123–1134. <https://doi.org/10.22092/ijfs.2018.114725>.